7

# Thermal Conduction Across Ferroelectric Phase Transitions: Results on Selected Systems

Jacob Philip
*Department of Instrumentation and STIC, Cochin University of Science and Technology*
*India*

## 1. Introduction

A *ferroelectric* phase transition represents a special class of structural phase transition characterized by the appearance of a spontaneous polarization in the material. Above the Curie temperature the transition often follows a diverging differential dielectric response or permittivity $\varepsilon$, which varies with temperature in an approximate Curie-Weiss manner $\varepsilon = C/(T-T_0)$, where $T_0$ is the Curie-Weiss temperature, which is equal to the Curie temperature $T_c$ for a continuous transition. The crystalline phase which undergoes transformation to the ferroelectric form at $T_c$ is the *paraelectric* one. Below $T_c$, in the absence of an applied field, there are at least two directions along which a spontaneous polarization can develop. To minimize the depolarizing fields different regions of the crystal polarize in each of these directions, each volume of uniform polarization being called a *domain*. The resulting *domain structure* usually results in a near complete compensation of polarization and the crystals consequently exhibit very small pyroelectric effects until they are poled by the application of a field.

A ferroelectric transition is usually associated with the condensation of a *soft* (or low-frequency) mode of lattice motion at the Brillouin-zone centre. Structural transitions triggered by zone-centre soft modes are generally termed *ferrodistortive*, and in this sense ferroelectrics constitute a subgroup of the class of *ferrodistortive* transitions. This subgroup involves the condensation of a polar or optically active mode whose condensation causes the appearance of a long rage polar order. If the transition is strongly first order then mode softening may not occur to a significant degree, and in this situation, there is also a possibility that the large polarization which sets in discontinuously at $T_c$ may not be reversible, or the low temperature phase may be pyroelectric only. Ferroelectric transitions are categorized as being either *displacive* or *order-disorder* in character. This distinction is generally made in terms of whether the paraelectric phase is microscopically nonpolar (displacive) or only nonpolar in a macroscopic or thermally averaged sense (order-disorder). The displacive or order-disorder character is often defined in terms of the dynamics of the phase transition, as to whether the soft mode is a propagating or diffusive type respectively. The displacive or propagating soft mode is a damped optic phonon, representing small quasi-harmonic motion about the mean position, while the diffusive soft mode represents large amplitude thermal hopping motion between the domain wells.

Although most ferroelectrics are ferrodistortive (common examples being barium titanate, sodium nitrite, and triglycine sulphate) some are not. To understand this it is necessary to recognize that, because of the existence of coupling between modes, it is not a necessary

condition for ferroelectricity that a zone centre polar mode should be driving the instability. Sometimes a driving antidistortive mode can couple directly or indirectly to a zone centre polar mode and upon condensation induce a small spontaneous polarization in an indirect fashion. In this case the primary order parameter is antidistortive in character while the spontaneous polarization is said to be a secondary order parameter of the transition. There can of course be only one primary order parameter (at least for a continuous or near continuous transition), but there may be many induced or secondary order parameters resulting from couplings to the primary order parameter. All the known antiferroelectrics (examples: lead zirconate, ammonium dihydrogen phosphate etc.) are intrinsically antidistortive, although one can conceive of a ferrodistortive antiferroelectric as one having an antiparallel arrangement of electric dipoles occurring within a primitive cell of the higher-symmetry phase. Such a phase is characterized by the condensation of an antipolar zone-centre soft mode.

Once the importance of coupling between polar modes and other modes has been recognized it is clear that, via the piezoelectric interaction (or coupling to acoustic modes), a spontaneous strain will be virtually a universal characteristic of ferroelectrics since all ferroelectrics are piezoelectric. If this strain can be switched by application of stress then an obvious parallel in elastic terms exists with ferroelectricity. This property is termed ferroelasticity, and a crystal is said to be ferroelastic when it has two or more orientation states in the absence of mechanical stress (and electric field) and can be shifted from one to another of these states by mechanical stress. Intrinsic ferroelastic transitions are associated with the condensation of long-wavelength acoustic phonons and many are known.

The optical and acoustic phonon modes involved in ferroelectric and ferroelastic phase transitions can be probed with Brillouin light scattering and ultrasonic techniques. When phonon modes soften, the involved elastic constants undergo anomalous variations which get reflected in ultrasound velocity and attenuation. Elaborate reviews on these subjects have appeared in literature (Luthi & Rehwald, 1980; Cummins, 1990). Other popular techniques used to probe modes in ferroelectrics are dielectric spectroscopy (Grigas, 1996) and neutron scattering (Dorner, 1981). A number of books and reviews on these subjects have appeared in literature (Lines & Glass, 1977). Though technique like measurement of thermal conductivity across phase transition can reveal information about the coupling between ferroelectric soft modes and thermal phonons, not many measurements have appeared in literature on this. The few measurements that have appeared in literature have used the well established steady-state methods of measuring thermal conductivity (Dettmer et al., 1989).

There are several ferroelectrics that undergo successive phase transitions with *incommensurate phases* (I-phase) from a symmetrical paraelectric to an incommensurate phase at *Ti* and then from the incommensurate phase to a commensurate polar phase at $T_c$ (Cummins, 1990, Blinc & Levanyuk, 1986). This phase transition sequence can be qualitatively described in terms of the phenomenological Landau theory of phase transitions (Toledano & Toledano, 1987). The appearance of an I-modulated structure can be observed experimentally as satellite peaks in X-ray or neutron diffraction patterns. In the I-phase, at temperatures close to *Ti*, the I-modulation wave is harmonic, but as the temperature approaches *Tc*, the ideal crystal can be considered as a system of equally spaced commensurate constant-phase domains separated by narrow phase varying regions, i.e., phase solitons. The presence of these modulation waves can influence heat conduction in ferroelectric crystals in two distinctive ways. As has been shown earlier, an interaction

manifested in sound attenuation exists between the acoustical waves and the I-modulation waves in the I-phase (Levanyuk et al., 1992; Lebedev et al., 1992). The usual expression for the thermal conductivity in an insulating crystal is given by

$$\lambda = \frac{1}{3} C \cdot \overline{v} \cdot l \tag{1}$$

where $C$, $\overline{v}$ and $l$ denote the specific heat, group velocity, and mean free path for phonons, respectively (Ashcroft & Mermin, 1976). The incommensurate modulation waves can affect the mean free path and, consequently, can cause an anomalous variation of thermal conductivity in the I-phase. Another possibility is that the modulation waves may participate directly in heat conduction as carriers. In this case, one would expect the modulation waves to enhance the thermal conductivity by the sliding motion in addition to causing the usual phonon scattering effect. The effect of sliding modulation waves on thermal conductivity has been investigated earlier within a phenomenological approach (Levanyuk et al., 1992). In spite of the fact that measurement of thermal properties across transition points is highly relevant to understand the coupling between modes, only limited experimental work has appeared on this in literature.

## 2. Overview of thermal properties across ferroelectric phase transitions

In the few measurements of the variations of thermal conductivity near ferroelectric phase transitions reported in literature, steady state methods have been employed. One of the first measurements was on $BaTiO_3$ by Mante & Volger (1967). Their results show dips in thermal conductivity at temperatures corresponding to phase transition points. The results are explained in terms of mode conversion near the transition points. The low lying temperature dependant optical phonon branches can get zero energy at zero wave-vector, which causes permanent polarization of the crystal. Near the transition temperature the optical branches have energies comparable to those of the acoustic branches which usually transport the heat. This influences the number of scattering processes in which optical phonons participate, resulting in a reduction of the conductivity due to acoustic branches. In case transverse optical phonon branch shows enough dispersion and is not scattered too much, one can expect additional conductivity which might compensate for the effect of decreased conduction by the acoustic phonons.

Thermal conductivities and specific heat capacities of a wide spectrum of ferroelectrics, $BaTiO_3$, $PbTiO_3$, $KNbO_3$, $KTaO_3$, $NaNbO_3$ and $Pb(Mg_{1/3}Nb_{2/3})O_3$ (PMN) single crystals have been measured from 2 to 390 K (Tachibana et al., 2008). Pronounced jumps are found at structural transitions in $BaTiO_3$ and $KNbO_3$. A low-temperature anomaly from soft optical phonons is observed in $KTaO_3$. For PMN and $NaNbO_3$, glass-like behaviour is observed in both thermal conductivity and heat capacity measurements. The glass-like behaviour in $NaNbO_3$ is associated with the phase separation phenomena which have been reported in earlier studies. Thermal analysis techniques such as differential scanning calorimetry (DSC) have been employed by several researchers to probe ferroelectric phase transitions (Setter & Cross, 1980, Podlojenov et al., 2006).

Belov & Jeong (1998) have reported thermal conductivity measurements for two ferroelectric crystals, $(NH4)_2BeF_4$ and $Rb_2ZnCl_4$, with incommensurate phases. It is found that anomalies exist in the thermal conductivities of these crystals in the I-phases. I-modulation waves cause anomalies in the heat transport processes by scattering of heat carrying phonons

rather than by their direct participation as heat carriers. They have employed the steady-state technique for their measurements. Comparatively large samples, of size typically greater than 5 $mm^3$, are needed for these techniques in order to avoid boundary effects. Moreover, comparatively large rises in temperature are often necessary to obtain a reasonably high signal to-noise ratio, which lead to considerable temperature gradients being set up in the sample. These drawbacks make these techniques unsuitable for studying critical thermal conductivity behaviour near phase transitions.

Thermal wave measurements based on a photothermal effect, such as the photothermal deflection technique, photoacoustic method and photopyroelectric measurement do not disturb the thermal equilibrium of the sample during transitions. In these techniques one measures the thermal diffusivity, rather than thermal conductivity. Thermal diffusivity measurements do not suffer from heat losses from the sample during measurements and hence are more accurate than a direct measurement of thermal conductivity by the steady state method. With a proper choice of boundary conditions, photothermal techniques make a simultaneous measurement of thermal diffusivity and thermal effusivity possible, from which the thermal conductivity and specific heat capacity can be extracted. The photopyroelectric technique has been used earlier to measure the variations of thermal conductivity and heat capacity of a few crystalline solids as they undergo phase transitions with temperature (Marinelli et al., 1990; Zammit et al., 1988; Mandelis et al., 1985).

## 3. The photopyroelectric technique

Complete characterization of the thermal properties of a material requires the determination of the thermal transport properties such as the thermal conductivity as well as the specific heat capacity. Techniques for high resolution measurement of specific heat capacity are well established (Kasting et al., 1980; Thoen et al., 1982). It has been shown that photothermal techniques allow simultaneous measurement of specific heat capacity $c_p$ and thermal conductivity $\lambda_s$ (Marinelli et al., 1990). The photoacoustic technique has been used for the simultaneous determination of the thermal diffusivity, thermal conductivity and heat capacity of liquid-crystalline compounds (Zammit et al., 1988). A somewhat similar technique has been used for measuring the thermal diffusivity and heat capacity of solids at room temperature using a photopyroelectric (PPE) detector (Mandelis et al., 1985; John et al., 1986). This technique enables simultaneous determination of thermal diffusivity, thermal effusivity, thermal conductivity and heat capacity as a function of temperature. Moreover, this technique allows studies of critical behaviours of thermal parameters when the material undergoes a transition. Marinelli et al. (1990) developed a technique to determine thermal diffusivity, thermal conductivity and heat capacity simultaneously at low temperatures with a pyroelectric detector kept in vacuum. At temperatures above room temperature, the boundary conditions involved in the theory of this method are not easy to satisfy, so that application of the method can lead to errors in measurement.

A photothermal technique for the simultaneous determination of the thermal conductivity and specific heat capacity near solid state phase transitions using a pyroelectric detector kept in contact with a thermally thick backing medium has been developed by Menon & Philip (2000). The PPE technique has some distinct advantages, such as its simplicity, good sensitivity and ability to perform nondestructive probing, over other photothermal methods. In this measurement the sample is heated by a modulated light source on one side and the temperature oscillations on the opposite side of the sample are detected with a

pyroelectric detector, supported on a thermally thick conductive backing. Since the PPE signal depends on properties of the detector which are also temperature dependent, an accurate temperature calibration of the system must be carried out. The advantage of a thermally thick backing is that there will be sufficient heat exchange between the heated pyroelectric detector and the backing, so that signal fluctuations are reduced to a minimum. This method can, in principle, be adapted to all temperature ranges for all samples and is not limited by the thermal properties of the sample.

The PPE effect is based on the use of a pyroelectric transducer to detect the temperature rise due to periodic heating of a sample by induced light. The temperature variations in the detector give rise to an electrical current, which is proportional to the rate of change of the average heat content, given by (Mandelis & Zver, 1985)

$$i_d = P\,A\left(\frac{\partial\theta(t)}{\partial t}\right) \tag{2}$$

where $P$ is the pyroelectric coefficient of the detector, $A$ is the area of the detector and

$$\theta(t) = \left(\frac{1}{L_d}\right)\int_0^{L_d}\theta(x,t)\,dx \tag{3}$$

is the spatially averaged temperature variation over the thickness of the detector, $L_d$.

For a thermally thick sample with $\mu_s < L_s$, and a thermally thick pyroelectric detector with $\mu_d < L_d$, where $\mu_s$ and $\mu_d$ are the thermal diffusion lengths of the sample and detector respectively, the expressions for the PPE amplitude and phase give expressions for the values of the thermal diffusivity $\alpha_s$ and effusivity $e_s$ which allow a simultaneous determination of the thermal conductivity and heat capacity if the density $\rho_s$ of the sample is known. The expressions for the temperature dependent PPE amplitude and phase under the above conditions are given by (Menon & Philip, 2000)

$$V(f,T) = \left(\frac{I_o\eta_s A R_d}{L_d\sqrt{\left[1+\left(f/f_c\right)^2\right]}}\right)\left(\frac{P(T)}{\rho_d(T)c_{pd}(T)}\right)\frac{\exp\left(-\left\{\sqrt{\pi f/\alpha_s}\right\}L_s\right)}{\left(\frac{e_s(T)}{e_d(T)}+1\right)} \tag{4a}$$

$$\varphi(f,T) = -\tan^{-1}\left(\frac{f}{f_c}\right) - \left(\sqrt{\pi f/\alpha_s(T)}\right)L_s \tag{4b}$$

where $T$ is the temperature and $c_{pd}$ and $\rho_d$ are the heat capacity (at constant pressure) and density of the detector respectively. $f_c$ is the characteristic frequency at which the sample goes from a thermally thin to thermally thick regime. From these two expressions it is clear that the thermal diffusivity $\alpha_s$ of the sample can be calculated from the phase of the PPE signal, which when substituted into the expression for the PPE amplitude, gives the thermal effusivity of the sample. From these the thermal conductivity and heat capacity of the sample can be calculated from the following relations:

$$\lambda_s(T) = e_s(T)\sqrt{\alpha_s(T)} \tag{5a}$$

$$c_{ps}(T) = \frac{e_s(T)}{\rho_s(T)\sqrt{\alpha_s(T)}} \tag{5b}$$

A temperature calibration of the PPE detector is necessary here as all the parameters in equations (4*a*) and (4*b*) are temperature dependent. All the thermal parameters can be calculated as functions of the sample temperature, provided that the temperature dependences of the parameters of the pyroelectric detector are known.

## 4. Experimental methods in PPE measurements

A sample set-up of the type shown in Fig. 1 is generally used for these measurements (Menon & Philip, 2000). A 120 mW He - Cd laser of $\lambda$ = 442 nm, modulated by a mechanical chopper, has been used as the optical heating source. A 28 $\mu$m thick film of PVDF with pyroelectric coefficient $P$ = 0.25 ×10$^{-8}$ V cm$^{-1}$ K$^{-1}$ at room temperature has been used as the pyroelectric detector. The sample is attached to the pyroelectric detector with a thermally very thin layer of a heat sink compound whose contribution to the signal is negligible. The pyroelectric detector attached to the sample is placed on a thermally thick backing medium (copper) which satisfies the boundary condition specified above. The frequency of modulation of the light is kept high enough to ensure that the PVDF film, the sample and the backing medium are all thermally thick. The signal output is measured with a lock-in amplifier. The sample-detector-backing assembly is enclosed in a chamber whose temperature can be varied and controlled as desired. Measurements as a function of temperature have been made at a low heating rate with special care near transition points. A block diagram of the experimental set up is shown in Fig. 2 for illustration.

The experimental set up and procedure should be calibrated and tested to ensure that even minor variations in heat capacity and thermal conductivity do get reflected in the measurements. Practically one measures the PPE amplitude and phase as function of modulation frequency, limiting the frequency to low values so that the sample, detector and backing are all thermally thick. From the amplitude and phase variations one can determine the thermal effusivity and thermal diffusivity following equations (4a) and (4b) respectively. From the values of thermal diffusivity and thermal effusivity, the values of thermal conductivity and specific heat capacity can be determined following equations (5a) and (5b).

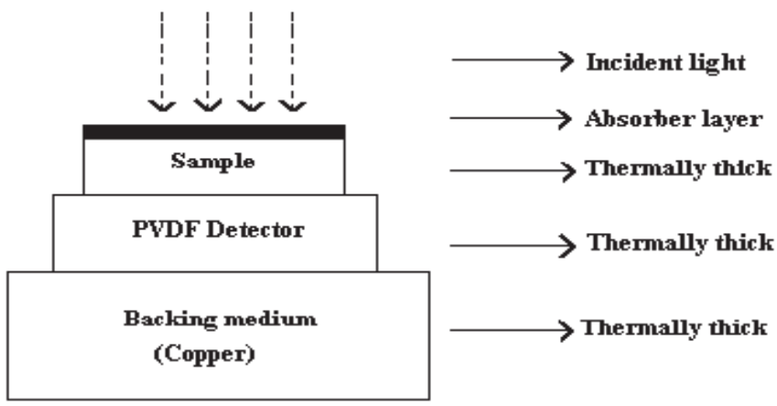


Fig. 1. The sample configuration for the photopyroelectric set-up

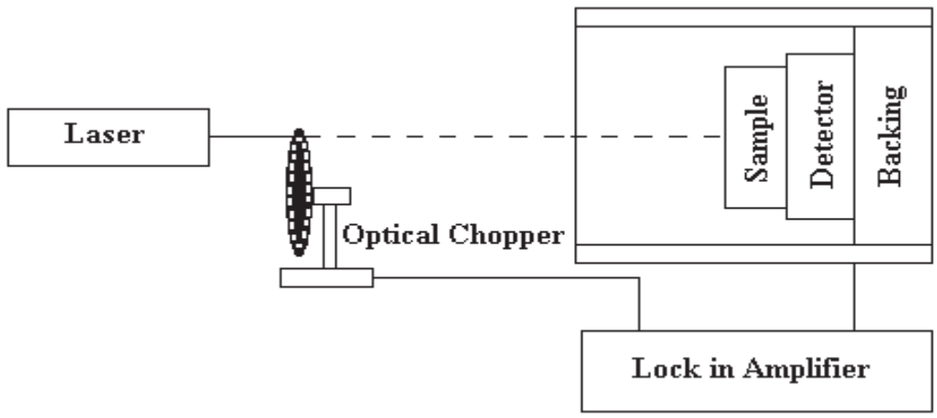


Fig. 2. Block diagram of the experimental set-up used for PPE measurements

Practically one measures the photopyroelectric signal amplitude and phase as function of modulation frequency. One will have inverse frequency dependence for the amplitude and phase beyond the critical frequency when the boundary conditions assumed are satisfied. A fitting of the variations of PPE amplitude and phase with the relations connecting thermal diffusivity and effusivity with phase and amplitude respectively enables one to determine the thermal diffusivity and effusivity. Typical variations of PPE amplitude and phase with modulation frequency obtained during PPE measurements in $K_2SeO_4$ are shown in figures 3a and 3b respectively. The peaks in the curves correspond to characteristic modulation frequency for the sample.

## 5. Results on specific systems and discussion

The variations in the thermal properties of the ferroelectric crystal Triglycine sulphate (TGS) were reported by Menon & Philip (2000). TGS crystals undergo a para–ferroelectric phase transition at 49.4°C. This crystal has a monoclinic structure at room temperature. Platelets of the crystal of sub-millimeter thickness were cut with faces normal to *a*, *b* and *c* axes so that the direction of propagation of thermal waves was along one of the axes. A very thin layer of carbon black was coated onto the illuminated surface of the sample to enhance its optical absorption. Measurements were carried out as a function of temperature from room temperature (26°C) to 55°C. The thermal thickness of the sample in these experiments was verified by plotting the PPE amplitude and phase against modulation frequency at a number of temperatures between room temperature and 55°C. The variations of the PPE amplitude and phase as functions of temperature were measured keeping the modulation frequency fixed at 40 Hz. From these, the thermal diffusivity ($a_s$) and effusivity ($e_s$) along the *b* axis of TGS were determined as functions of temperature. These are shown in Fig. 4a. The temperature variations of $\lambda_s$ along the *b* axis and $c_{ps}$ were also determined (shown in Fig. 4b). The heat capacity results presented in Fig. 4b agree with those already reported in the literature (Strukov & Levanyuk 1998). Their results showed that thermal conductivity along the *b* axis has a minimum value at the transition point. Measurements of the thermal diffusivity or conductivity along *a*- and *c*- axes did not reveal any anomaly at the phase transition temperature. This was in agreement with thermal diffusivity measurements along these axes reported earlier (Gaffar et al., 1987).

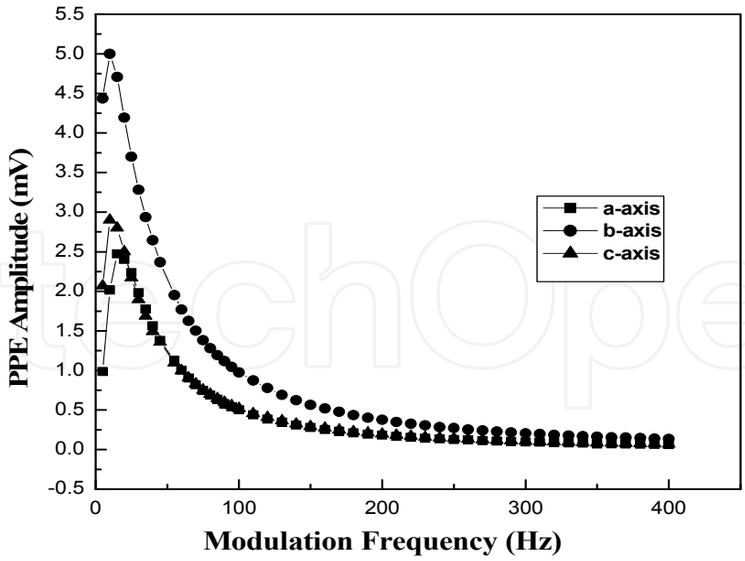


Fig. 3. (a) Frequency dependence of the photo-pyroelectric amplitudes along the three principal axes of $K_2SeO_4$ at room temperature (Philip & Manjusha, 2009)

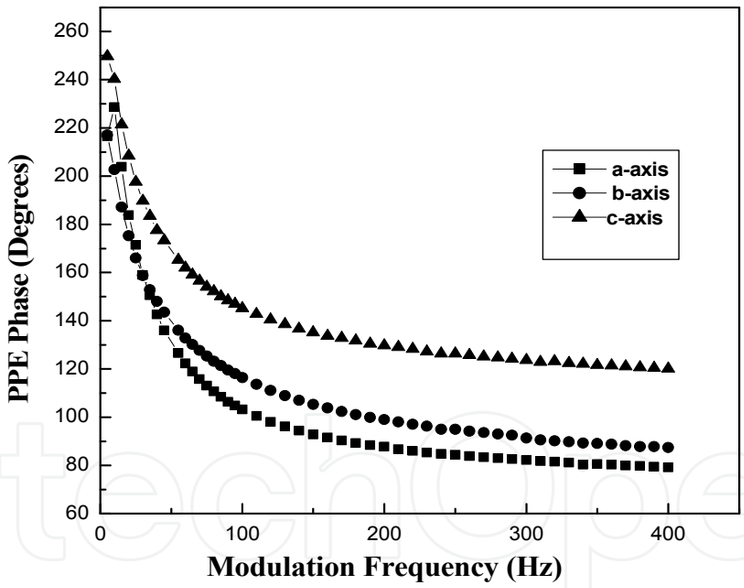


Fig. 3. (b) Frequency dependence of the photopyroelectric phases along the three principal axes of $K_2SeO_4$ at room temperature (Philip & Manjusha, 2009)

Ferroelectric crystals, which exhibit incommensurate phase transitions include ammonium fluroberrylate (Iizumi & Gesi, 1977), potassium selenate (Iizumi et al., 1977), sodium nitrite (Yamada et al., 1963), thiourea (Goldsmith & White, 1959) etc. Thiourea, with the chemical formula SC $(NH_2)_2$, undergoes successive phase transitions at 169 K ($T_1$), 176 K ($T_2$), 180 K ($T_3$) and 202 K ($T_4$). Among the five phases (called I, II, III, IV and V) in the order of increasing temperature, two of them (I and III) are ferroelectric and a superlattice structure appears in the II, III and IV phases (Elcombe & Tayler, 1968). The crystal structure in the

room temperature phase V above $T_4$ is orthorhombic and belongs to the space group $D^{16}_{2h}$-*Pbnm* with four molecules per unit cell ($Z$ = 4). The phase I below $T_1$ is a ferroelectric one having spontaneous polarization along the *b*-axis, whose crystal structure is also orthorhombic with four molecules per unit cell ($Z$ = 4).

In the three intermediate phases, II, III and IV between $T_1$ and $T_4$, Shiozaki (1971) analyzed X-ray reflection spectra and concluded that the crystal has an in-commensurate structure. According to his analysis, just above $T_4$ the crystal has a superstructure along the *c*-axis with a period about eight times as large as that of phase IV. The period of the super structure increases as temperature decreases. So in the vicinity of $T_1$, the period is about ten times as large and at $T_1$ the crystal transforms to the ferroelectric phase I, where the period of the unit cell of the prototype is restored. More elaborate descriptions of the properties of thiourea are available in literature (Wada et al., 1978, Moudden et al., 1978, Mc Kenzie, 1975a, Mc Kenzie, 1975b, Delahaigue et al., 1975, Chapelle & Benoit, 1977).

The thermal properties described above during the incommensurate-commensurate phase transition in thiourea were measured employing PPE technique (Menon & Philip, 2003). Measurements have been done along the three principal directions of thiourea and the observed anisotropy in thermal transport is discussed. The crystals were cut with their faces normal to the [100], [010] and [001] directions of the crystallographic *a*-, *b*- and *c*-axes respectively. Measurements were carried out illuminating the three cut sample faces so that the propagation of the thermal wave is along one of the symmetry directions. The variations of thermal conductivity and heat capacity as functions of temperature across the transition temperatures were measured as outlined above.

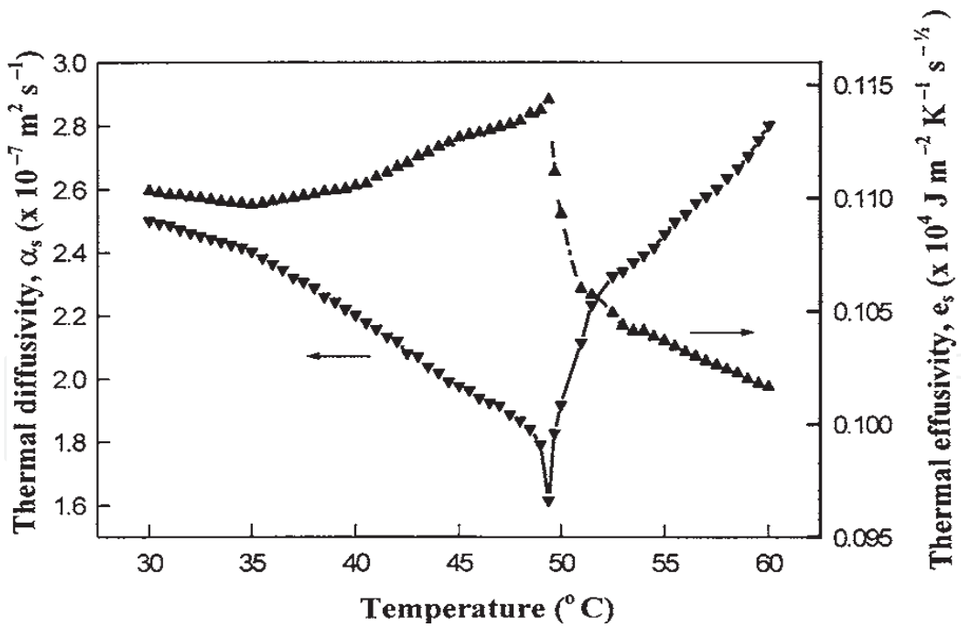


Fig. 4. (a) Variations of the thermal diffusivity (inverted triangles) and thermal effusivity (triangles) with temperature for TGS along the *b* axis (Menon & Philip, 2000)

It was seen that both PPE amplitude and phase clearly reflect the three successive phase transitions in thiourea. The maximum anomaly was at $T_1$, the temperature at which transition to an in-commensurate phase took place. Anomalies were measured along *a, b*

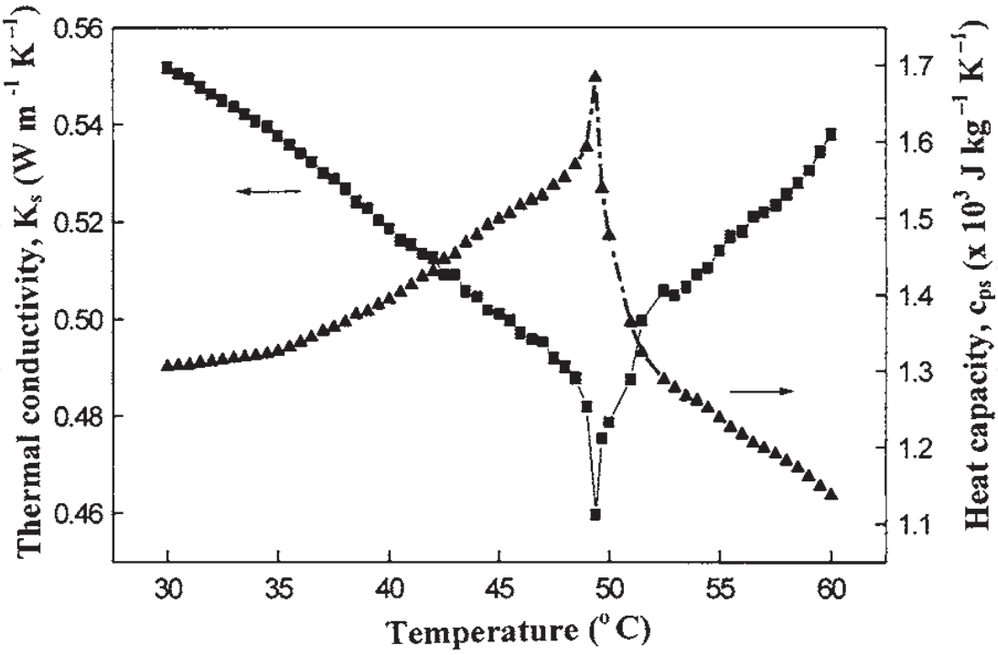


Fig. 4. (b) Variations of the thermal conductivity (inverted triangles) and heat capacity (triangles) with temperature along the *b*-axis (Menon & Philip, 2000)

and *c* directions at the same temperatures. The maximum variation was seen along the *b*-direction, the direction in which the crystal possesses spontaneous polarization in the ferroelectric phase. Fig. 5a shows the variations of thermal diffusivity and thermal effusivity with temperature along the *b*-axis of thiourea single crystal. As can be seen in this figure, thermal diffusivity shows a decrease with temperature, with distinct minima at the three phase transition points at $T_1$ ≈169 K, $T_3$ ≈176K and $T_4$ ≈ 202 K, in agreement with the already reported values of transition temperatures. Thermal effusivity exhibits an inverse behaviour. It increases with temperature, with sharp peaks occurring at the transition temperatures. Taking into account the various uncertainties of the measurement, the overall uncertainty in the values of α and *e* are estimated to be less than 5%. Similar anomalies with smaller magnitudes have been obtained for the *a*- and *c*-directions as well.

Figure 5b shows the variation of heat capacity of thiourea with temperature. As can be seen in this figure, the three transitions get clearly reflected in the temperature variation of heat capacity as clear anomalies at the transition points. These heat capacity values agree with the values reported by earlier workers (Hellwege & Hellwege, 1969). As can be seen, there is no direction dependence for heat capacity. Figure 5c shows the temperature variation of thermal conductivity along the three symmetry directions (*a*, *b* and *c*) of thiourea. The thermal conductivity exhibits significant anisotropy, as is evident from Fig. 5c. The three transitions get clearly reflected in the thermal conductivity variations as well. The maximum anomaly at the transition temperatures is seen along the *b*-axis. The maximum thermal conduction occurs in the direction of predominant covalent bonding, which is along the *b*-axis in thiourea. This is the direction of spontaneous polarization in this crystal.

Dicalcium Lead Propionate (DLP, with chemical formula $Ca_2Pb$ $(C_2H_5COO)_6$, belonging to the family of double propionates, is ferroelectric below 333K along the c- axis (Nakamura et al 1965). It undergoes a para to ferro electric phase transition at 333K ($Tc_1$), which is a second

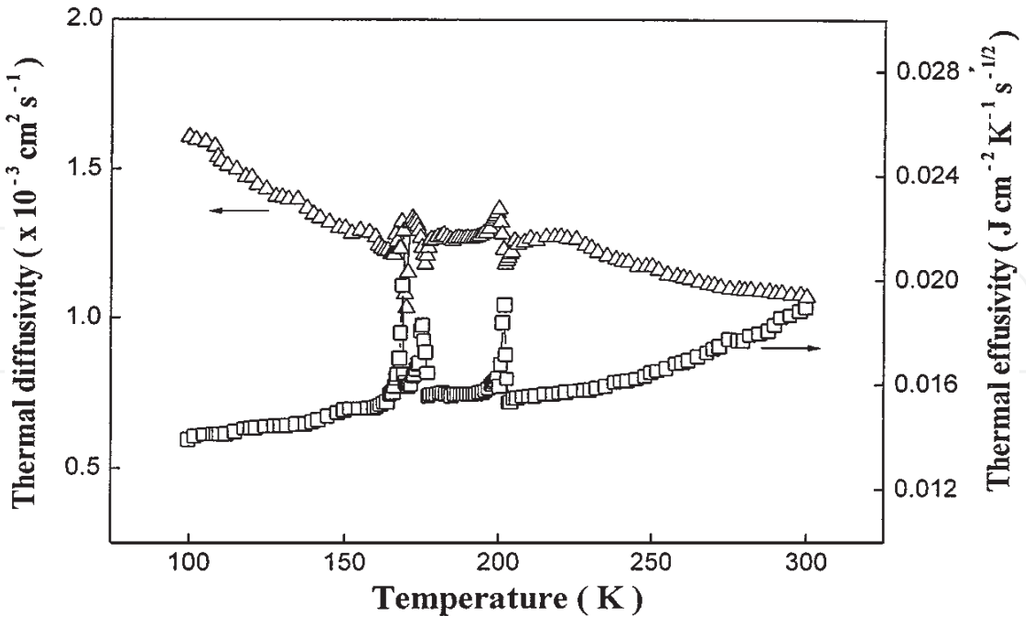


Fig. 5. (a) Temperature variations of thermal diffusivity and thermal effusivity along the *b*-axis of thiourea single crystal. Similar variations to a lesser extend were exhibited by *a*- and *c*-directions (Menon & Philip, 2003)

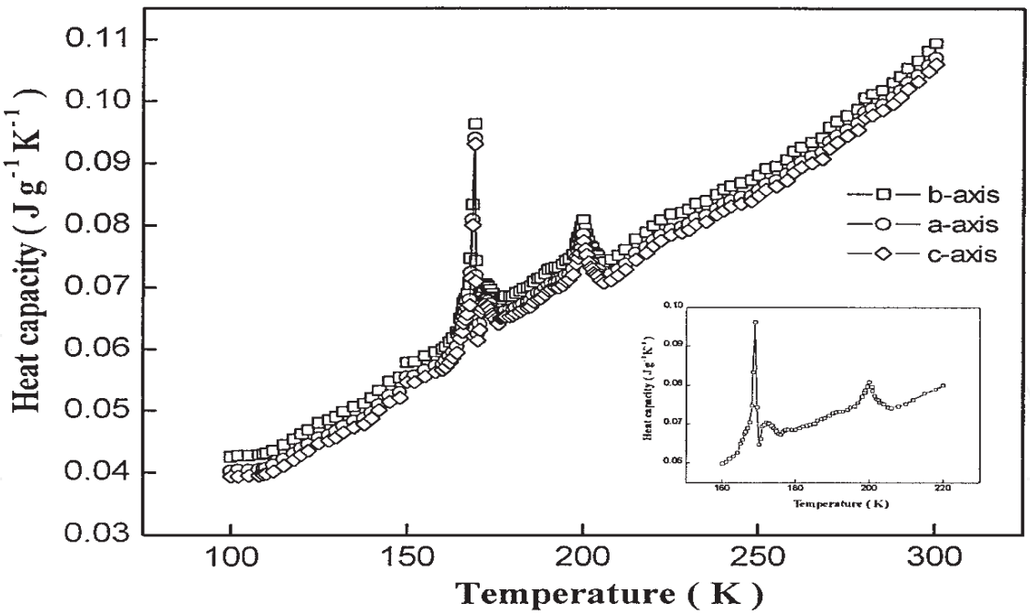


Fig. 5. (b) Temperature variation of heat capacity along three principal directions of thiourea single crystal. The inset shows the variation of heat capacity between 160 K and 220 K along the *b*-axis (Menon & Philip, 2003)

order one. Upon decreasing the temperature further, it undergoes another phase transition at 191K ($Tc_2$), which is first order. The transition at $Tc_1$ is associated with the movement of the ethyl group ($C_2H_5$) (Nakamura et al., 1978), but the one at $Tc_2$ is still not understood

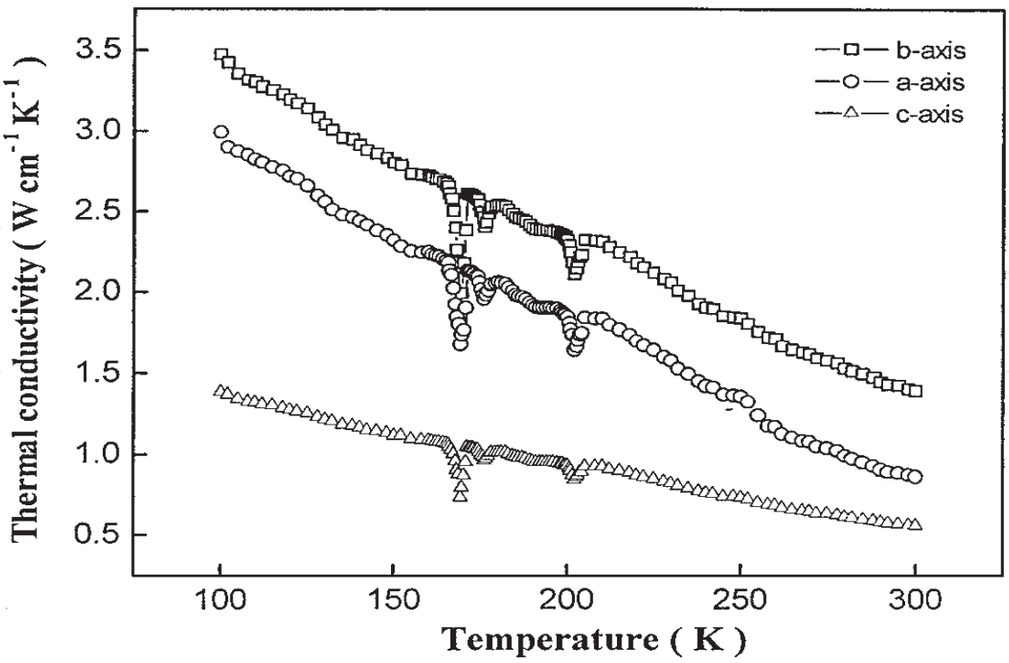


Fig. 5. (c) Temperature variations of thermal conductivity along three principal directions of thiourea single crystal. (Menon & Philip, 2003)

well. Even below this transition temperature the material continues to remain ferroelectric. Based on the measurement of the hydrostatic pressure dependence of the crystal structure of DLP above and below the respective phase transitions, Gesi & Ozawa (1975) have proposed that the phases above and below $Tc_2$ are isomorphous to each other. However, on the basis of polarizing microscopic observations and dielectric constant measurements, Gesi (1984) has concluded that the two phases above and below $Tc_2$ are not isostructural.

The crystal structure of DLP is tetragonal at room temperature (Ferroni & Orioli, 1959). The lead atoms are located at *4a* positions and calcium atoms at *8b* positions. Studies on the pyroelectric properties of DLP associated with its phase transitions have led to the conclusion that DLP crystal between $Tc_1$ and $Tc_2$ is tetragonal and polar, the point group in this phase being $C_4$ or $C_{4v}$ (Osaka et al., 1975). Raman, infrared and dielectric properties of this crystal has been studied by earlier workers (Nagae et al., 1976, Takashige et al., 1978). The phase diagrams of mixed crystal system DSP-DLP, where DSP stands for Dicalcium Strontium propionate, has been determined by Nagae et al. (1976) from dielectric and dialatometric measurements. Nage et al., (1976) have reported Raman scattering spectra of DSP and DLP between 73 and 423K. They concluded that both phase transitions of these two materials are of the order – disorder type since no soft modes are observed, implying that these transitions are most probably isomorphous. Takashige et al. (1978) have reported the piezoelectric and elastic properties of ferroelectric DLP over a wide temperature region, including the ferroelectric-paraelectric phase transition point ($Tc_1$).

Even though the specific heat of DLP was reported way back in 1965 (Nakamura et al., 1965), other thermal properties such as thermal conductivity were not. Moreover, systematic thermal analysis following thermogravimetry or scanning calorimetry through $Tc_1$ and $Tc_2$ have not been reported. These measurements in DLP through the transition temperatures have been reported by Manjusha & Philip (2008). These authors have reported thermal

transport properties of the sample, thermal diffusivity, effusivity, conductivity and specific heat capacity as a function of temperature following PPE technique. The anisotropy in thermal diffusivity/conductivity along the principal axes as well as their variation through these transition temperatures was measured.

The variations of thermal properties, shown in figures 6a and 6b, clearly indicate that the thermal properties undergo anomalous variations during phase transitions at 191 K and 333 K. In general, the thermal diffusivity and thermal conductivity show an anomalous decrease during transitions, whereas the heat capacity shows a corresponding anomalous increase. Being an electrical insulator crystal, the major contribution to the heat capacity of DLP is from lattice phonons and the electronic contribution to heat capacity is very small. As the phonon modes undergo variations due to mode instability at the transition points, they absorb excess energy giving rise to enhancement in heat capacity. This is found to get reflected in the DSC curve as well. Again, during the transitions, the phonon mean-free path increases, resulting in a decrease in thermal resistance or a corresponding increase in thermal diffusivity and thermal conductivity. The anisotropy in thermal conductivity is not very high for this crystal. The maximum thermal conduction occurs along the *c*-axis, which is the direction of spontaneous polarization.

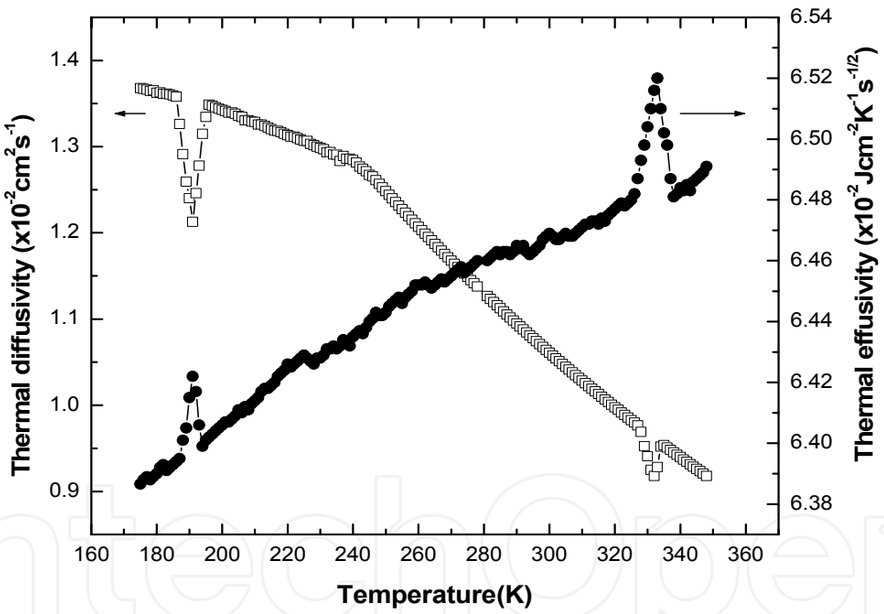


Fig. 6. (a) Variation of thermal diffusivity and thermal effusivity for DLP crystal, cut with faces normal to the c-axis (Manjusha & Philip, 2008)

Many experimental and theoretical studies have been carried out by different workers to understand the mechanisms of phase transitions in potassium selenate *($K_2SeO_4$)* single crystals, ever since the discovery of ferroelectricity and successive phase transitions in this crystal (Aiki et al., 1969). With the occurrence of ferroelectric phase, this material undergoes an incommensurate phase (IC phase) transition. Potassium selenate undergoes three successive phase transitions at temperatures $T_1$ = 745 K, $T_2$ = 129.5 K and $T_3$ = 93 K (Aiki *et al* 1969). The crystal exhibits hexagonal structure in phase I, with space group $D_{46h}$ *(P63/mmc)* (Shiozaki *et al* 1977*)*, which changes to an orthorhombic structure (phase II) with space

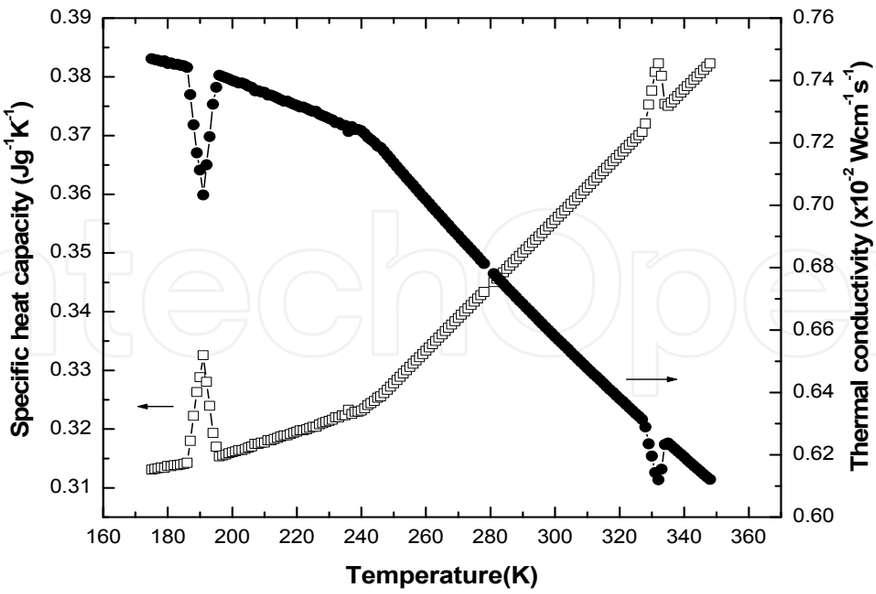


Fig. 6. (b) Variation of thermal conductivity and specific heat capacity for DLP crystal, cut with faces normal to the c-axis (Manjusha & Philip, 2008)

group $D_{16\ 2h}$ (*Pnam*) at $T_1$ (Kalman *et al* 1970). Then, phase II changes into an incommensurate one (phase III) at $T_2$ (Iizumi et al., 1977); this is a second order phase transition. It undergoes an IC phase transition at $T_3$, below which the crystal is commensurate and ferroelectric with a small spontaneous polarization along the *c* direction.

Many experimental studies such as dielectric measurements (Aiki et al., 1969, Aiki et al., 1970), X-ray and neutron diffraction (Iizumi et al., 1977; Ohama, 1974; Terauchi et al., 1975), ESR (Aiki, 1970), Raman and Brillouin scattering (Wada et al., 1977a; Wada et al., 1977b; Yagi et al., 1979), ultrasound velocity, attenuation and dispersion studies (Hoshizaki et al., 1980; Shiozaki, 1977) etc have been reported near $T_2$ and $T_3$. The variations in specific heat capacity and thermal expansion of $K_2SeO_4$ in the low temperature phase have also been reported before (Aiki et al., 1970; Gupta et al., 1979). Thermal expansion along the *c*-axis exhibits a discontinuity at the incommensurate to commensurate transition. Specific heat measurements show anomalies at $T_2$ and $T_3$, indicating that the transition at $T_2$ is second order and that the one at $T_3$ is first order (Aiki et al., 1970). In spite of all these measurements reported at temperatures $T_3$ and $T_2$, only very few experimental results have been reported near $T_1$ ( Unruh et al., 1979; Inoue et al., 1979; Cho & Yagi, 1980; Gupta et al., 1979) because of the inherent difficulties involved in carrying out precision experiments at high temperatures. The variation of the specific heat capacity across the structural transition at $T_1$ has not been reported so far for this material. More experimental data are still required for a better understanding of the high temperature phase of this material.

The thermal diffusivity, thermal conductivity and heat capacity of $K_2SeO_4$ as it goes through the IC phase between 129.5 and 93 K have been measured by Philip & Manjusha (2009). The anisotropy in thermal conductivity along the three principal directions of this crystal and its variation with temperature are brought out and discussed by these authors. Differential scanning calorimetric (DSC) measurements across the high temperature phases have been carried out to determine anomalies in enthalpy during transition from phase I to phase II, and

the calorimetric ratio method adopted to determine the variation of specific heat capacity with temperature across the high temperature transition point $T_1$. The results from PPE and calorimetric measurements have been combined to plot the variation of specific heat with temperature through all the four phases of $K_2SeO_4$, and the results discussed below.

PPE measurements were done at temperatures between 85 and 300 K. Thermal diffusivity and effusivity along the *c* axis, plotted against temperature are shown in Fig. 7a. From the diffusivity and effusivity values, the values of the thermal conductivity and specific heat capacity have been computed, and these are plotted in Fig 7b. Since the values of these thermal parameters for *a* and *b* axes are not very different from the corresponding values obtained for the *c*-axis, they are not reproduced. It can be noticed that the thermal conductivity along the *c* axis, which is the direction of spontaneous polarization for this crystal, is slightly more than that along *a*- or *b*-axis at all temperatures. The anisotropy in thermal conductivity is small and decreases as the temperature is lowered. The variations along the *c* axis clearly indicate that the thermal properties undergo anomalous variation during phase transitions at 93 and 129.5 K. Thermal conductivity and heat capacity exhibit maxima at the phase transition temperatures 93 and 129.5 K. Moreover, there is an overall enhancement in thermal conductivity in the IC phase of $K_2SeO_4$ between 93 and 129.5 K. The maxima in thermal conductivity at the phase transition temperatures can be explained in terms of the increase in phonon mean free path or decrease in phonon–phonon and phonon–defect collision rates. Again, the anomalous variation in specific heat capacity is due to softening of phonon modes and the corresponding enhanced contribution of phonon modes to the specific heat capacity.

The IC phase in $K_2SeO_4$ has been observed experimentally as satellite peaks in the x-ray and neutron diffraction patterns (Iizumi et al., 1977). In the IC phase of $K_2SeO_4$ at temperatures close to $T_2$, the incommensurate modulation wave is pure harmonic. But as the temperature approaches $T_3$, nonlinear phase modes, which are equally spaced commensurate constant phase domains separated by narrow phase varying regions called phase solitons, emerge. The presence of these modulation waves or phase solitons can influence heat conduction in ferroelectric crystals in two different ways, as outlined below.

The phase solitons can affect the mean free path of thermal phonons via scattering and hence can cause anomalous variation of thermal conductivity in the IC phase. Another possibility is that the modulation waves themselves can act as heat carriers, resulting in an enhancement in thermal conductivity. Whether the thermal conductivity increases or decreases during an IC phase transition depends on which factor dominates in the process. One can isolate thermal conductivity enhancement in the IC phase by computing the value of $(\lambda - \lambda_{bg})$ where $\lambda$ is the total thermal conductivity and $\lambda_{bg}$ is the background thermal conductivity in the absence of occurrence of IC modulation. In general, for an insulating crystal, $\lambda_{bg}$ follows an inverse temperature ($T$) variation.

The theory of heat conduction in a ferroelectric crystal with a two-component order parameter has been developed by Levanyuk and co-workers (Levanyuk et al., 1992). The theory considers heat conduction along the modulation axis of a system that undergoes IC phase transition. According to this, the thermal conductivity due to phase solitons is given by

$$\lambda = \lambda_{bg} + \left( c_0^2 T \rho^2 / \gamma \right) \tag{6}$$

where $c_0$ and $\gamma$ are constants and $\rho$ is the magnitude of the order parameter. One can see that the phase solitons enhance the thermal conductivity of $K_2SeO_4$ in the IC phase. It has also

been shown that the enhancement in thermal conductivity is related to the excess specific heat $c_e$ due to order parameter fluctuation as

$$\frac{\partial(\lambda - \lambda_{bg})}{\partial T} \approx c_e \tag{7}$$

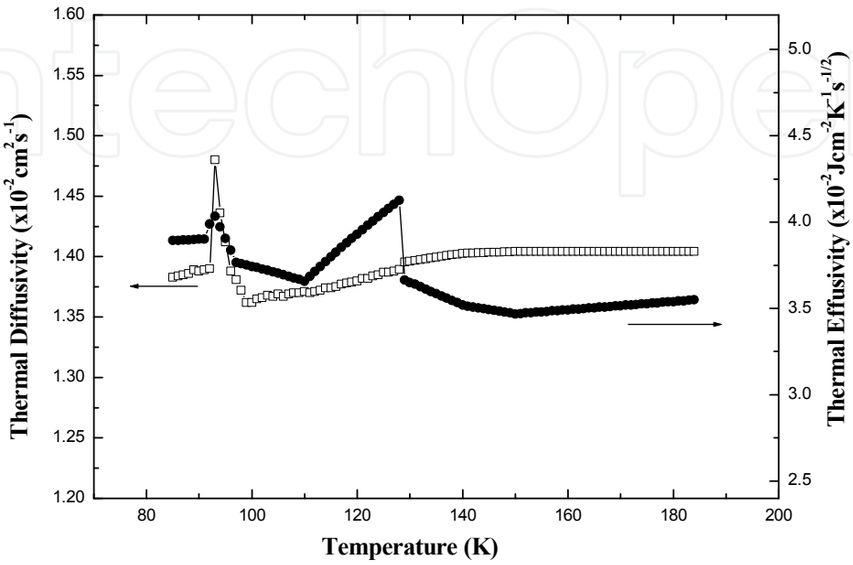


Fig. 7. (a) Variation of the thermal diffusivity and thermal effusivity along the *c*- axis of $K_2SeO_4$ (Philip & Manjusha, 2009)

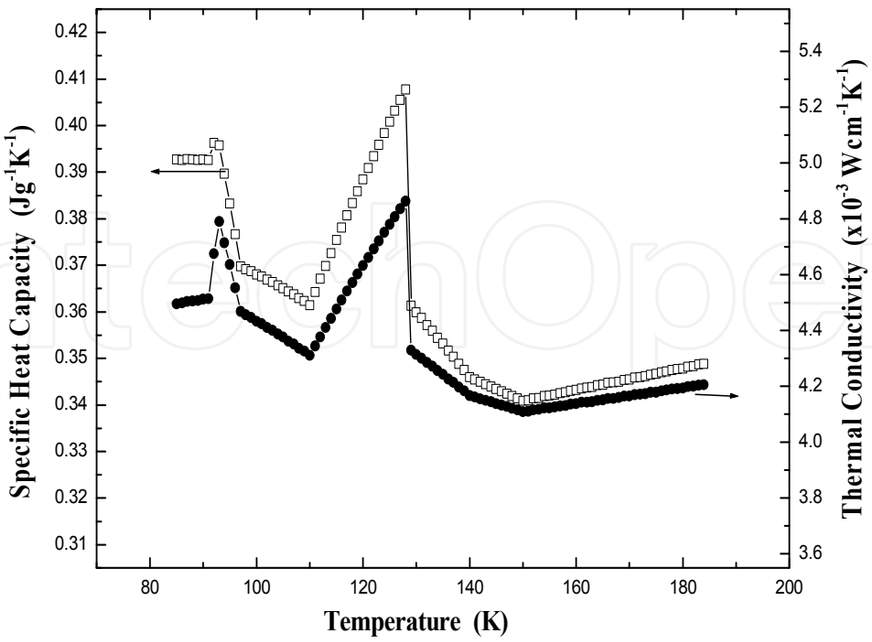


Fig. 7. (b) Variations of the thermal conductivity along the *c* axis and specific heat capacity of $K_2SeO_4$ (Philip & Manjusha, 2009)

This explains the enhancement in specific heat in the modulation phase of the crystal. Even without the effects expressed in equations (6) and (7), the modulation waves can cause anomalies in ($\lambda - \lambda_{bg}$) by strongly scattering the heat carrying phonons. In the IC phase between 93 and 129.5 K, one can note that the background thermal conductivity and the specific heat decrease gradually as the temperature increases. This variation of thermal conductivity is normal for a solid, but the variation of the specific heat is just opposite to the normal behaviour for solids. This can be attributed to the increase in the heat capacity of the modulation waves with decrease in temperature. As the system approaches the low temperature commensurate phase, it becomes more and more ordered, resulting in a decrease in entropy or increase in heat capacity. The modulation waves are so strong in the IC phase that the contribution of modulation waves to the overall heat capacity of the system is much more than the contribution of normal phonon modes to heat capacity. This results in an overall increase in heat capacity as the temperature decreases in the IC phase. The DSC curve during the heating cycle shows a clear peak occurring at 745 K, indicating that the phase transition at this temperature is endothermic. The variation of specific heat capacity with temperature up to a temperature well above 745 K has been determined by the DSC ratio method. These results have been combined with the results shown in figure 7b to plot the variation of heat capacity with temperature encompassing all the four phases of $K_2SeO_4$. This is shown in Fig. 8. So figure 8 contain the variation of specific heat of $K_2SeO_4$ through all the three transition temperatures $T_1$, $T_2$ and $T_3$ (and through all the four phases). The anomalous variation of heat capacity during transitions can be understood as due to softening of the phonon modes and the corresponding enhanced contribution of phonon modes to the specific heat capacity of the system.

In order to estimate the quantity of excess heat capacity due to the structural phase transition at 745 K, the contribution of the normal heat capacity shall be subtracted from the measured molar heat capacity. The background lattice heat capacity was approximated by a third-order polynomial. The excess of the molar heat capacity $\Delta Cp$ was plotted against ($T - T_c$) and it is found to have a shape typical for a continuous phase transition. At $T = T_c$, $\Delta Cp$ is found to be $0.112 \pm 0.003$ J $K^{-1}$ $mol^{-1}$. The specific heat critical exponent α was obtained from the slope of log ($\Delta Cp$) versus log ($T - Tc$). The value of α is found to be $-0.0853 \pm 0.0002$, which is close to zero. This value for α is typical for a mean field model of a phase transition (Strukov & Levanyuk, 1998). The Landau theory gives a simple relation between the excess entropy and the order parameter $P_s$ (spontaneous polarization), given by

$$\Delta S(T) = -(1/2)[A_0 P_s^2] \tag{8}$$

One can acquire more information about the nature of the phase transition from the excess entropy $\Delta S$. The most direct way to determine $\Delta S$ is from a measurement of the excess heat capacity as a function of temperature:

$$\Delta S(T) = \int_{T_o}^{T} \frac{\Delta C_p}{T} dT \tag{9}$$

The transition entropy has been calculated from the above equation, and is obtained as $\Delta S = 0.49 \pm 0.03$ J $K^{-1}$ $mol^{-1}$. This is typical of a structural phase transition. However, this is much smaller than the transition entropy predicted by the order-disorder model in the mean field theory. Other mechanisms such as tunnelling may have to be taken into account to reduce this discrepancy with experiment.

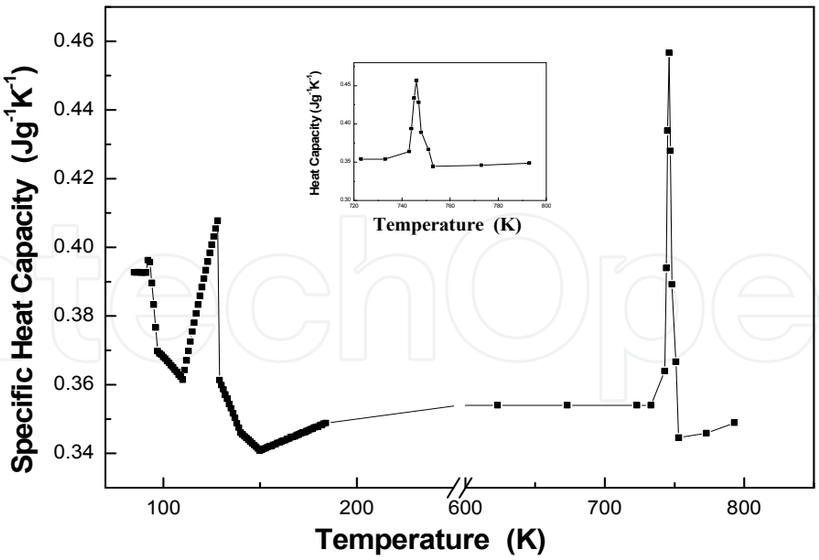


Fig. 8. Variation of the specific heat capacity with temperature through all the four phases of $K_2SeO_4$. The inset shows the variation close to the high temperature transition point (Philip & Manjusha, 2009)

## 6. Conclusions

The results presented in the above section show that a photothermal technique such as the photopyroelectric technique is a convenient and sensitive one to measure thermal conductivity and specific heat capacity of ferroelectric crystals as they undergo phase transitions. Photothermal techniques do not suffer from the disadvantages of steady state techniques. In a photothermal technique one actually measures the thermal diffusivity which is independent of heat losses from the sample. With a careful control of the sample boundary conditions the PPE technique has proven to be a sensitive and convenient one to measure thermal transport properties of solids that undergo ferroelectric phase transitions.

Even though not much attention has been paid to the measurement of thermal properties for probing phase transitions in solids, it is now more and more obvious that thermal transport measurements yield critical information to throw more light on fine features of ferroelectric transitions, particularly those involving incommensurate modulation of the lattice. Measurement of fine features of the variations of thermal conductivity and specific heat capacity with temperature, without disturbing the system, provides valuable information about the interactions involved in the processes.

## 7. Acknowledgements

The author thanks University Grants Commission (New Delhi) and Cochin University of Science and Technology for financial support provided for the publication of this article.

## 8. References

Aiki, H. (1970). ESR Study of γ-Irradiated $K_2SeO_4$, *J. Phys. Soc. Japan* 29, 379-88

Aiki, K.; Hukuda, K.; Koga, H. & Kobayashi, T. (1970). Dielectric and thermal study of $K_2SeO_4$ transitions, *J. Phys. Soc. Japan* 28, 389-94

Aiki, K.; Hukuda, K. & Matumura, O. (1969). Ferroelectricity in $K_2SeO_4$, *J. Phys. Soc. Japan* 26, 1064

Ashcroft, N. W. & Mermin, N. D. (1976). *Solid State Physics* (Holt, Rinehart and Winston, New York) Chap. 25

Badarinath, K. V. S. & Radhakrishna, S. (1984). Studies on the ferroelectric-paraelectric transition of dicalcium lead propionate, *J. Mat. Sci. Lett.* 3, 575-577

Belov, A. & Jeong, Y. H. (1998). Anomalous heat conduction in ferroelectric crystals with incommensurate phases, *J. Korean Phys. Society* 32, 452 - 455

Bhat, S. V.; Dhar, V. & Srinivasan, R. (1981). ESR studies on phase transitions in double propionates, *Ferroelectrics* 39, 1167

Blinc, R. & Levanyuk, A. P. (1986). *Incommensurate Phases in Dielectrics 1 & 2*, (North-Holland, Amsterdam)

Chapelle, J. P. & Benoit, J. P. (1977). Raman study of external frequencies of thiourea with temperature, *J. Phys. C: Solid State Phys.* 10, 145-51

Cho, M. & Yagi, T. (1980). Brillouin scattering study of the Hexagonal-Orthorhombic phase transition in $K_2SeO_4$, *J. Phys. Soc. Japan* 49, 429-430

Cummins, H. Z. (1990). Experimental studies of structurally incommensurate crystal phases, *Phys. Reports* 5 & 6, 211

Delahaigue, A.; Khelifa, B. & Jouve, P. (1975). Soft mode in thiourea by Raman measurements, *Phys. Stat. Solidi (b)* 72, 585-89

Dettmer, E. S.; Romenesko, B. M.; Charles Jr., H. K.; Carkhuff, B. G. & Mewll, D. J. (1989). Steady-state thermal conductivity measurements of AlN and SiC substrate materials, *IEEE Transactions on Components, Hybrids, and Manufacturing Technology*, 12, 543-548

Dorner, B. (1981). Investigation of structural phase transformations by inelastic neutron scattering in Structural Phase Transitions I (editors: K A Muller & H. Thomas, in *Topics in Current Physics* Vol. 23, Springer-Verlag, Berlin)

Elcombe, M. & Tayler, J. C. (1968). A neutron diffraction determination of the crystal structures of thiourea and deuterated thiourea above and below the ferroelectric transition, *Acta Cryst. A* 24, 410 -20

Ferroni, E. & Orioli, P. (1959). Zur kristallstruktur von $PbCa_2$ $(CH3CH2COO)_6$, *Z. Krist.* 111, 362

Gaffar, M. A.; Mebed, M. M. & El-Fadl, A. (1987). Thermal Diffusivity of Pure and Doped TGS Crystals, Phys. Status Solidi a 104, 879- 884

Gesi, K. (1984). Reinvestigation of pressure-Induced II-III transitions in Ferroelectric $Ca_2Sr(C_2H_5COO)_6$ and $Ca_2Pb(C_2H_5COO)_6$, *J. Phys. Soc. Japan* 53, 1602-1605

Gesi, K. & Ozawa, K. (1975). Effect of Hydrostatic pressure on the phase transitions in Ferroelectric $Ca_2Sr(C_2H_5COO)_6$ and $Ca_2Pb(C_2H_5COO)_6$, *J. Phys. Soc. Jpn.* 39, 1026-1031

Goldsmith, G. J. & White, J. G. (1959). Ferroelectric behavior of Thiourea, *J. Chem. Phys*. 31, 1175-1187

Grigas, J. (1996). *Microwave dielectric spectroscopy of ferroelectrics and related materials* (Gordon and Breach Publishers)

Gupta, S. S.; Karan, S. & Gupta, S. P. S. (2000). Growth and defect characterization in single crystals of Ferroelectric Ammonium Sulphate, *Japan J. Appl. Phys.* 39, 2736-40

Hellwege, K. H. & Hellwege, A. M. (editors) *Landolt - Bornstein New Series* (1969) Vol 3 ed: (Springer – Verlag, New York) p. 477

Hoshizaki, H.; Sawada, A.; Ishibashi, Y.; Matsuda, T. & Hatta, I. (1980). Ultrasonic study of $K_2SeO_4$ in the temperature range of the incommensurate phase transition, *Japan. J. Appl. Phys.* 19, L324-26

Inoue, K.; Suzuki, K.; Sawada, A.; Ishibashi, Y. & Takagi, Y. (1979). A test of centrosymmetry of the hexagonal phase in $K_2SeO_4$, *J. Phys. Soc. Japan* 46, 608-10

Iizumi, M.; Axe, J. D.; Shirane, G. & Shimaoka, K. (1977). Structural phase transformation in $K_2SeO_4$, *Phys. Rev. B* 15, 4392

Iizumi, M. & Gesi, K. (1977). Incommensurate pháse in $(ND_4)_2BeF_4$, *Solid State Commun* 22, 37-39

John, P. K.; Miranda, L. C. M. & Rastogi, A. C. (1986). Thermal diffusivity measurement using the photopyroelectric effect, *Phys. Rev. B* 34, 4342-4345

K´alm´an, A.; Stephens, J. S. & Cruickshank, D. W. J. (1970). The crystal structure of $K_2SeO_4$, *Acta Crystallogr.* B 26, 1451-
54

Kasting, G. B.; Garland, C. W. & Lushington, K. J. (1980). Critical heat capacity of octylcyanobiphenyl (8CB) near the nematic-smectic A transition, *J. de Physique* 41, 879

Lebedev, N. I.; Levanyuk, A. P.; Minyukov, S. A. & Vallade, M. (1992). Elastic anomalies at structural phase transitions: a consistent perturbation theory. II. Two-component order parameter including the case of incommensurate phase, *J. Phys. I (France)* 2, 2293-97

Levanyuk, A. P.; Minyukov, S. A. & Vallade, M. (1992). Elastic anomalies at structural phase transitions: a consistent perturbation theory. I. One component order parameter, *J. Physique I (France)* 2, 1949-63

Lines, M. E. & Glass, A. M. (1977). *Principles and Applications of Ferroelectrics and related Materials* (Clarendon Press, Oxford, 1977)

Luthi, B. & Rehwald, W. (1981). Ultrasonic studies near structural phase transitions, in *Structural Phase Transitions I* (ed: K A Muller & H Thomas, in *Topics in Current Physics* Vol. 23, Springer-Verlag, Berlin)

Mandelis, A; Care, F.; Chan, K. K. & Miranda, L. C. M. (1985). Photopyroelectric detection of phase transitions in solids, *Appl. Phys. A* 38, 117

Mandelis, A. & Zver, M. M. (1985). Theory of photopyroelectric spectroscopy of solids, *J. Appl. Phys.* 57, 4421- 4430

Manjusha, M. V. & Philip, J. (2008). Thermal properties of Dicalcium Lead Propionate across the prominent transition temperatures, *Ferroelectrics Letters* 35, 107 - 118

Mante, A. J. H. & Volger, J. (1967). The thermal conductivity of $BaTiO_3$ in the neighborhood of its ferroelectric transition temperatures, *Phys. Letters* 24A, 139

Marinelli, M. ; Murtas, F.; Mecozzi, M. G.; Zammit, U.; Pizzoferrato, R.; Scudieri, F.; Martellucci, S. & Marinelli, M. (1990). Simultaneous determination of specific heat, thermal conductivity and thermal diffusivity at low temperature via the photopyroelectric technique, *Appl. Phys.* A 51, 387-393

Mc Kenzie, D. R. (1975a). Neutron and Raman study of the lattice dynamics of deuterated thiourea, *J. Phys. C: Solid State Phys.* 8, 2003

Mc Kenzie, D. R. (1975b). The antiferroelectric transition in thiourea studied by thermal neutron scattering, *J. Phys. C: Solid State Phys.* 8, 1607

Menon, C. P. & Philip, J. (2000). Simultaneous determination of thermal conductivity and heat capacity near solid state phase transitions by a photopyroelectric technique, *Meas. Sci. Technol*. 11, 1744–1749

Menon, C. P. & Philip, J. (2003). Thermal properties of Thiourea studied using Photopyroelectric technique, *Ferroelectrics* 287, 63-70

Moudden, A. H. ; Denoyer, F. ; Benoit, J. P. & Fitzgerald, W. (1978). Inelastic neutron scattering study of commensurate-incommensurate phase transition in thiourea, *Solid State Commun.* 28, 75

Nagae, Y. ; Wada, M. ; Ishibashi, Y & Takagi, Y. (1976). Raman Scattering Spectra of $Ca_2Sr(C_2H_5CO_2)_6$ and $Ca_2Pb(C_2H_5CO_2)$, *J. Phys. Soc. Jpn.* 41, 1659-1662

Nakamura, N.; Akamura, H.; Suga, H.; Chihara, H. & Seki, S. (1965). Phase transitions in crystalline divalent metal dicalcium propionates I. Calorimetric and dielectric investigations of strontium and lead dicalcium propionates, *Bull. Chem. Soc. Jpn.* 8, 1779-1787

Nakamura, N.; Suga, H. ; Chihara, H & Seki, S. (1978). Phase transitions in crystalline divalent metal dicalcium propionates. II. Proton magnetic resonance investigation, *Bull. Chem. Soc. Jpn*. 41, 291-296

Ohama, N. (1974). Superstructure of potassium selenate $K_2SeO_4$, *Mater. Res. Bull.* 9, 283-88

Osaka, T; Makita, Y & Gesi, K. (1975). Pyroelectricity of dicalcium lead propionate associated with its phase transitions, *J. Phys. Soc. Jpn.* 38, 292

Philip, J. & Manjusha, M. V. (2009). Thermal transport across incommensurate phases in potassium selenate: Photo-pyroelectric and calorimetric measurements, *J. Phys.: Condens. Matter* 21, 045901

Podlojenov, S; Stade, J; Burianek, M & Mühlberg, M. (2006). Study on the ferroelectric phase transition in potassium lithium niobate (KLN), *Cryst. Res. Technol.* 41,344 – 348

Setter, N. & Cross, L. E. (1980). The contribution of structural disorder to diffuse phase transitions in ferroelectrics, *J. Materials Science* 15, 2478-2482

Shiozaki, Y. (1971). Satellite X-ray scattering and structural modulation of thiourea, *Ferroelectrics* 2, 245-60

Shiozaki S; Sawada A; Ishibashi, Y & Takagi, Y. (1977). Hexagonal-orthorhombic phase transition and ferroelasticity in $K_2SO_4$ and $K_2SeO_4$, *J. Phys. Soc. Japan* 43, 1314-19

Standnicka, K.; Glazer, A. M. & Bismayer, U. (1990). The phase diagram of dicalcium strontium/lead propionate, *Phase transitions* 27, 73-80

Strukov, B. A. & Levanyuk, A. P. (1998). *Ferroelectric Phenomena in Crystals* (Springer, Berlin)

Sunil Misra, K. & Jerzak, S. (1989). $Mn_{2+}$ EPR study of phase transitions in dicalcium lead propionate $Ca_2Pb(C_2H_5COO)_6$: Determination of critical exponent below the ferroelectric phase transition and comparison with EPR studies on $Ca_2Ba(C_2H_5COO)_6$ and $Ca_2Sr(C_2H_5COO)$, *Phy. Rev. B* 39, 2041-2050

Tachibana, M.; Kolodiazhnyi, T. & Takayama-Muromachi, E. (2008). Thermal conductivity of perovskite ferroelectrics, *Appl. Phys. Letters* 93, 092902

Takashige, M.; Hirotsu, S.; Sawada, S. & Humano, K. (1978). Piezoelectric and elastic properties of Dicalcium lead propionate, *J. Phys. Soc. Jpn.* 45, 558-564

Terauchi, H; Takenaka, H & Shimaoka, K. (1975). Structural Phase Transition in $K_2SeO_4$, *J. Phys. Soc. Japan* 39, 435-39

Thoen, T; Marynissen, H & Van Dael, W.(1982). Temperature dependence of the enthalpy and the heat capacity of the liquid-crystal octylcyanobiphenyl (8CB) *Phys. Rev. A* 26, 2886-2905

Toledano, J. & Toledano, P. (1987). *The Landau theory of phase transitions* (World Scientific, Singapore), Chapter 5

Unruh, H. G.; Eller, W. & Kirf, G. (1979). Spectroscopic and dielectric investigations of $K_2SeO_4$, *Phys. Status Solidi a* 55, 173-80

Wada, M.; Sawada, A.; Ishibashi, Y. & Takagi, Y. (1977). Raman scattering spectra of $K_2SeO_4$, *J. Phys. Soc. Japan* 42, 1229-34

Wada, M.; Sawada., A; Ishibashi., Y. & Takagi, Y. (1978). Raman scattering spectra of SC $(NH_2)_2$, *J. Phys. Soc. Jpn.* 45, 1905-10

Wada, M.; Uwe, H.; Sawada, A.; Ishibashi, Y.; Takagi, Y & Sakudo, T (1977). The lower frequency soft-mode in the ferroelectric phase of $K_2SeO_4$, *J. Phys. Soc. Japan* 43, 544

Yamada, Y.; Shibuya, I. & Hoshino, S. (1963). Phase transition in $NaNO_2$, *J. Phys. Soc. Japan* 18, 1594-1603

Yagi, T.; Cho, M. & Hidaka, Y. (1979). Brillouin scattering study of the paraelectric-incommensurate phase transition in $K_2SeO_4$, *J. Phys. Soc. Japan* 46, 1957-58

Zammit, U.; Marinelli, M.; Pizzoferrato, R.; Scudieri, F. & Martellucci, S. (1988). Photoacoustics as a technique for simultaneous measurement of thermal conductivity and heat capacity, *J. Phys. E: Sci. Instrum.* 21, 935-937

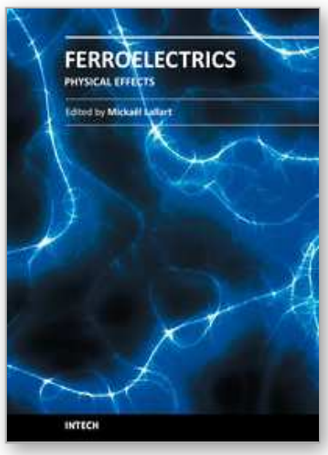


**Ferroelectrics - Physical Effects**

Edited by Dr. MickaÃ«l Lallart

ISBN 978-953-307-453-5
Hard cover, 654 pages
**Publisher** InTech
**Published online** 23, August, 2011
**Published in print edition** August, 2011

Ferroelectric materials have been and still are widely used in many applications, that have moved from sonar towards breakthrough technologies such as memories or optical devices. This book is a part of a four volume collection (covering material aspects, physical effects, characterization and modeling, and applications) and focuses on the underlying mechanisms of ferroelectric materials, including general ferroelectric effect, piezoelectricity, optical properties, and multiferroic and magnetoelectric devices. The aim of this book is to provide an up-to-date review of recent scientific findings and recent advances in the field of ferroelectric systems, allowing a deep understanding of the physical aspect of ferroelectricity.



INTECH
open science | open minds

**InTech Europe**
University Campus STeP Ri
Slavka Krautzeka 83/A
51000 Rijeka, Croatia
Phone: +385 (51) 770 447
Fax: +385 (51) 686 166
www.intechopen.com

**InTech China**
Unit 405, Office Block, Hotel Equatorial Shanghai
No.65, Yan An Road (West), Shanghai, 200040, China
中国上海市延安西路65号上海国际贵都大饭店办公楼405单元
Phone: +86-21-62489820
Fax: +86-21-62489821

IntechOpen